

Time- and Space-Efficient Regular Path Queries on Graphs

Diego Arroyuelo

Universidad Técnica Federico Santa María & IMFD
Santiago, Chile
darroyue@inf.utfsm.cl

Gonzalo Navarro

DCC, University of Chile & IMFD
Santiago, Chile
gnavarro@dcc.uchile.cl

Aidan Hogan

DCC, University of Chile & IMFD
Santiago, Chile
ahogan@dcc.uchile.cl

Javiel Rojas-Ledesma

DCC, University of Chile & IMFD
Santiago, Chile
jrojas@dcc.uchile.cl

ABSTRACT

We introduce a time- and space-efficient technique to solve regular path queries over labeled graphs. We combine a bit-parallel simulation of the Glushkov automaton of the regular expression with the ring index introduced by Arroyuelo et al., exploiting its wavelet tree representation of the triples in order to efficiently reach the states of the product graph that are relevant for the query. Our query algorithm is able to simultaneously process several automaton states, as well as several graph nodes/labels. Our experimental results show that our representation uses 3–5 times less space than the alternatives in the literature, while generally outperforming them in query times (1.67 times faster than the next best).

PVLDB Reference Format:

Diego Arroyuelo, Aidan Hogan, Gonzalo Navarro, and Javiel Rojas-Ledesma. Time- and Space-Efficient Regular Path Queries on Graphs. PVLDB, 15(X): XXX-XXX, 2022.
doi:XX.XX/XXX.XX

PVLDB Artifact Availability:

The source code, data, and/or other artifacts have been made available at <https://github.com/darroyue/Ring-RPQ>.

1 INTRODUCTION

A characteristic feature of graph databases is the ability to query over paths of arbitrary length [3]. This feature is typically supported as *regular path queries (RPQs)* [13, 36], which specify a regular expression that constrains matching paths. Consider the graph of Fig. 1 describing different means of transportation within Santiago de Chile. Edges are directed and labeled with the type of transportation (l1, l2 and l5 denote three metro lines). We can find pairs of locations reachable by metro with an RPQ $x \xrightarrow{(l1|l2|l5)^+} y$, where x and y are variables over the nodes of the graph, while the regular expression $(l1|l2|l5)^+$ will match paths of length one-or-more such that each edge has the label l1, l2 or l5. We may also fix one or both nodes in an RPQ, for example $\text{Baquedano} \xrightarrow{(l1|l2|l5)^+} y$ finds nodes reachable from Baquedano by metro.

This work is licensed under the Creative Commons BY-NC-ND 4.0 International License. Visit <https://creativecommons.org/licenses/by-nc-nd/4.0/> to view a copy of this license. For any use beyond those covered by this license, obtain permission by emailing info@vldb.org. Copyright is held by the owner/author(s). Publication rights licensed to the VLDB Endowment.

Proceedings of the VLDB Endowment, Vol. 15, No. X ISSN 2150-8097.
doi:XX.XX/XXX.XX

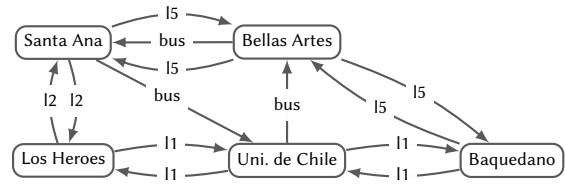


Figure 1: Santiago metro stations with metro lines and buses

While regular path queries have long been studied in theoretical works [13, 36], recently they have been included in practical query languages for graphs [3]. The SPARQL 1.1 [27] query language for RDF graphs includes *property paths* [31], which extend RPQs with inverse paths and negated edge labels. Oracle’s graph query language PGQL [49] also supports RPQs, as does the G-CORE query language [2] defined by the LDBC standardisation committee. The Cypher query language [19], supported by Neo4j, includes limited forms of RPQs (with Kleene-star and concatenation). In summary, RPQs have become a key feature in modern graph databases [3], and are frequently used: in an analysis of 208 million SPARQL queries issued to the Wikidata Query Service [34], Bonifati et al. [7] find that 24% of the queries use at least one RPQ/property path feature.

The problem of efficiently evaluating RPQs has been gaining increasing attention in recent years [1, 5, 12, 14, 17, 18, 24–26, 28–30, 32, 33, 35, 37, 38, 43–45, 47, 52–56]. The traditional algorithm – used, for example, in the theoretical literature to prove complexity bounds – is based on representing the regular expression of the RPQ as a non-deterministic finite automaton, defining the product graph of the data graph and the automaton, and then applying graph search on the product graph (BFS, DFS, etc.) [36]. While the product graph is potentially large, practical algorithms can avoid materialising it, and rather expand it lazily during navigation. Other more recent approaches propose the use of recursive queries [29, 55, 56], parallel [38] and distributed [12, 26, 35, 44, 54] frameworks, indexing techniques [18, 24, 32, 33], multi-query optimization [1], approximation [52], just-in-time compilation [47], etc., in order to efficiently evaluate RPQs. However, these works have mainly focused on improving efficiency in terms of time, but not space.

Our Contribution. We introduce a new technique to handle RPQs (with inverses) on labeled graphs that works on a recent compressed

representation of the graph called a ring [4]. The ring was introduced for handling multijoin queries in worst-case optimal time while using essentially the same space as a plain representation of all the triples (s, p, o) denoting edges $s \xrightarrow{p} o$ of the labeled graph. The ring represents those nodes and edge labels as a sequence in a convenient order called the Burrows-Wheeler Transform (BWT) [9] of the triples, and in turn represents the sequence using a wavelet tree data structure [23]. Our technique combines (1) the backward search capabilities of the BWT, (2) the ability of the wavelet trees to efficiently work on ranges of nodes or edge labels, and (3) the regularity of the Glushkov automaton [22] of the regular expression and the versatility of its bit-parallel simulation [42]. As a result, we efficiently navigate towards the nodes of the product graph that are involved in the solution of the RPQ, being able to process several NFA states and several graph nodes/labels simultaneously. Theorem 4.1 shows that we spend logarithmic time per node and edge of the product subgraph induced by the query. Our experimental results show that we obtain a time-competitive query solution within about twice the space of a compact data representation (because we need to duplicate all edges to handle reversed edges in the RPQs). This is still 3–5 times less than the space used by prominent alternative indexes that handle RPQs, while our index outperforms them in general: it was the fastest index on average in our benchmark, 1.67 times faster than Blazegraph, the second fastest index.

2 RELATED WORK

We now present related work on efficiently evaluating RPQs and related types of expressions, such as property paths in SPARQL.

Query planning. Various techniques have been proposed for evaluating path-based queries. Earlier works focused on evaluating shortest paths, such as the works on spatial networks Miao et al. [37], or reducing navigation to joins [25]. Later works began to focus on RPQs, coinciding with the standardisation of SPARQL 1.1.

Regarding navigation-based approaches, Koschmieder and Leser [30] propose to split an RPQ by its *rare labels*, i.e., labels with fewer than m edges where at least one such edge must be used in each path matching the RPQ; for example, given an expression $a^*/b/c^*$ (where \cdot^* denotes Kleene star and \cdot/\cdot concatenation), if b has few edges, the expression may be split into a^*/b and b/c^* to ensure more selective start/end points, and later joined. Nolé and Sartiani [44] evaluate RPQs using the concept of *Brzozowski derivatives*, whereby the regular expression is rewritten based on the symbols already read such that the rewritten expression matches suffixes that complete the path; for example, if the original expression is $a^*/b/c^*$, and we advance along an edge labeled b , then the derivative is c^* . Wang et al. [54] evaluate RPQs based on *partial answers* that can be connected, allowing for these answers to not only be prefixes, but also infixes and suffixes; for example, if the original expression is $a^*/b/c^*$, partial answers corresponding to a^* (prefix), b/c (infix) and c^* (suffix) can be generated in parallel and combined. Nguyen and Kim [43] split RPQs similarly to the “rare labels” strategy, but rather minimize the cost of the most costly sub-RPQ resulting from the split. Wadhwa et al. [52] compute approximate RPQ results using bidirectional random walks, where a forward walk begins from the source node, a backward walk begins from the target node, and walks that “meet” are reported as solutions.

Other approaches evaluate RPQs using recursive (query) languages. Dey et al. [14] evaluate RPQs using Datalog or recursive SQL queries; they further return *provenance* in the form of all edges involved in some or all matching paths. Yakovets et al. [55] likewise propose to translate property paths into recursive SQL queries, but note that the resulting queries can be complex and difficult to optimize. Jachiet et al. [29] propose an extended relational algebra with a transitivity/fixpoint operator, and describe how RPQs (more specifically, unions of conjunctive RPQs) can be translated to this algebra. Fionda et al. [17] propose *extended property paths*, which includes difference and intersection over paths, as well as the ability to express tests that constrain nodes along the path; non-recursive expressions are translated into SPARQL 1.1, while recursive expressions require a recursive extension of SPARQL.

Combining both navigational/automata and recursive/relational approaches, Yakovets et al. [56] propose hybrid “waveplans” that can mix operators from both algebras and thus can express novel query plans. Abul-Basher [1] propose a related framework called “swarmguide” for optimizing multiple RPQs at once, based on finding a maximum common sub-automaton for the RPQs, which can be evaluated and reused across RPQs using views.

Finally, a number of approaches leverage software or hardware acceleration techniques. Miura et al. [38] evaluate RPQs on top of field programmable gate arrays (FPGAs), which enable high degrees of parallelism; specifically, the RPQ is split into multiple “stages”, where sort–merge joins are applied on the FPGA to join results from different stages in a pipelined manner. Tetzl et al. [47] use just-in-time compilation techniques in order to generate native C++ code that directly evaluates the RPQ on the graph.

Indexing. Custom indexing approaches have also been proposed for optimizing RPQ evaluation. Gubichev et al. [24] extend RDF-3X with support for property paths using an indexing technique called FERRARI [46], based on encoding the transitive closure of the graph induced by a given edge label using (potentially overapproximated) intervals of node ids. Wang et al. [53] propose a predicate-based indexing scheme to evaluate RPQs over RDF graphs, where four orders are indexed – ps , pos , ps , po – in order to efficiently evaluate triple patterns with a fixed predicate. Fletcher et al. [18] propose a *k-path index* that indexes all paths of length up to k in a B⁺-tree, specifically indexing the word of the path, the source node, and the target node. Kuijpers et al. [32] describe the use of *k-path indexes* to optimize the evaluation of Cypher queries in the Neo4j graph database, while Liu et al. [33] use similar indexes, which they populate with frequent paths mined from the graph.

Other settings. We focus on evaluating RPQs over a static graph on a single machine. However, we briefly mention some other works on evaluating RPQs in other settings. A number of works have looked into enabling horizontal scale by evaluating RPQs over RDF graphs distributed/partitioned over multiple machines [12, 26, 35, 44, 54], sometimes using existing frameworks such as Pregel [44] or MapReduce [12]. Other works have explored the evaluation of property paths/RPQs over Linked Data in the decentralized setting, whereby RDF graphs on the Web are navigated dynamically while evaluating the RPQ [5, 28]. A recent work has explored the evaluation of RPQs over sliding windows of streaming graph data [45].

Novelty. We introduce a novel technique to evaluate RPQs (with inverses) that is efficient both in time and space. While some indexing schemes explore a time-space trade-off, they occupy space *additional* to representing and indexing the graph [46]. To the best of our knowledge, our approach is the first that can efficiently evaluate RPQs on a compressed representation of the graph, and the first to evaluate RPQs based on Glushkov automata [22], highlighting key advantages of this construction: It not only enables a more space-efficient bit-parallel simulation of the NFA [42], but also its transitions exhibit a regularity that is crucial to efficiently evaluating RPQs. The combination of the backward search capabilities of the BWT [9], the ability of the wavelet trees [23] to work on ranges of nodes/labels, and the regularity of Glushkov’s automaton, allow us to simulate the traversal of *only* the product subgraph induced by the RPQ (without spending time on outgoing edges). The bit-parallel simulation and the ability to work on ranges of nodes and labels further enable processing sets of nodes of the product graph *simultaneously*, thus speeding up the classical evaluation strategy.

3 BASIC CONCEPTS

3.1 Regular Path Queries

Let Σ denote a set of symbols. We define a (directed edge-labeled) graph $G \subseteq \Sigma \times \Sigma \times \Sigma$ to be a finite set of triples of symbols of the form (s, p, o) , denoting (subject, predicate, object). Each triple of G can be viewed as a labeled edge of the form $s \xrightarrow{p} o$. Given a graph G , we define the *nodes* of G as $V = \{x \mid \exists y, z, (x, y, z) \in G \vee (z, y, x) \in G\}$.

A *path* ρ from x_0 to x_n in a graph G is a string of the form $x_0 p_1 x_1 \dots p_n x_n$ such that $(x_{i-1}, p_i, x_i) \in G$ for $1 \leq i \leq n$. Abusing notation, we may write that $\rho \in G$ if ρ is a path in G . We call $\text{word}(\rho) = p_1 \dots p_n \in \Sigma^*$ the *word* of ρ .

We say that ε is a *regular expression*, and that any element of Σ is a regular expression. If E, E_1 and E_2 are regular expressions, we say that E^* (Kleene closure), E_1/E_2 (concatenation) and $E_1|E_2$ (disjunction) are also regular expressions. We may further use E^+ as an abbreviation for E^*/E , and E^\wedge as an abbreviation for $\varepsilon|E$.

We define by $\hat{\Sigma} = \{\hat{s} \mid s \in \Sigma\}$ the *inverses* of the symbols of Σ , and by $\Sigma^{\leftrightarrow} = \Sigma \cup \hat{\Sigma}$ the set of symbols and their inverses. We assume that $\Sigma \cap \hat{\Sigma} = \emptyset$ and that $s = \hat{(\hat{s})}$. We denote by $\hat{G} = \{(y, \hat{p}, x) \mid (x, p, y) \in G\}$ the *inverse* of a graph G , and by $G^{\leftrightarrow} = G \cup \hat{G}$ the *completion* of G . If E is a two-way regular expression, then so is \hat{E} (inverse). A two-way regular expression on Σ can be rewritten to a regular expression on Σ^{\leftrightarrow} .

Given a regular expression E , we denote by $L(E)$ the language of E , and we say that a path ρ *matches* E if and only if $\text{word}(\rho) \in L(E)$.

Let Φ denote a set of variables. Let $\mu : \Phi \rightarrow \Sigma$ denote a partial mapping from variables to symbols. We denote the domain of μ as $\text{dom}(\mu)$, which is the set of variables for which μ is defined. If E is a regular expression, $s \in \Phi \cup \Sigma$ and $o \in \Phi \cup \Sigma$, then we call (s, E, o) a *regular path query (RPQ)*. Let x_μ be defined as $\mu(x)$ if $x \in \text{dom}(\mu)$, or x otherwise. We define the *evaluation* of (s, E, o) on G as:

$$(s, E, o)(G) = \{\mu \mid \text{dom}(\mu) = \{s, o\} \cap \Phi \text{ and there exists a path } \rho \text{ from } s_\mu \text{ to } o_\mu \text{ in } G \text{ such that } \rho \text{ matches } E\}.$$

Example. Take the graph G of Fig. 1 and the RPQ $(x, (1|1|2|15)^+, y)$, where $x, y \in \Phi$ are variables. Infinitely many paths in G match the expression $(1|1|2|15)^+$, including (abbreviating node labels):

UCh 11 LH 11 UCh
UCh 11 LH 11 UCh 11 LH
Baq 11 UCh 11 LH 12 SA

and so forth. The evaluation of the RPQ on G will return all mappings such that x maps to the start node of some such path, and y maps to the end node of the same path. For example, from the first path, we will return a solution μ such that $\mu(x) = \text{UCh}$, $\mu(y) = \text{UCh}$, and μ is undefined for all other variables. The evaluation is finite as it can map x and y , at most, to all pairs of nodes in G .

If we instead consider $(\text{Baq}, (1|1|2|15)^+, y)$, where $\text{Baq} \in \Sigma$ and $y \in \Phi$, then its evaluation on G will return all mappings such that y maps to the end node of a path that starts with Baq . For example, from the third path listed previously, we would return μ such that $\mu(y) = \text{SA}$ and μ is undefined for all other variables.

Finally, the evaluation of $(\text{Baq}, (1|1|2|15)^+, \text{SA})$, where $\text{Baq}, \text{SA} \in \Sigma$, returns a single solution μ that is undefined for all variables; if SA were not reachable from Baq via a path matching $(1|1|2|15)^+$, then no solution would be returned. \square

If E is a two-way regular expression over Σ , $s \in V \cup \Phi$ and $o \in V \cup \Phi$, we call (s, E, o) a *two-way regular path query (2RPQ)*. We define the evaluation of the 2RPQ (s, E, o) on G as the evaluation of the RPQ (s, E', o) on G^{\leftrightarrow} , where E' is the rewritten form of E using only atomic inverses, and is thus a regular expression over Σ^{\leftrightarrow} .

3.2 Product Graph

One approach for evaluating an RPQ (s, E, o) on G involves computing the *product graph* of G [36]. Specifically, we first convert the regular expression E into a non-deterministic finite automaton (NFA) $M_E = (Q, \Sigma_E, \Delta, q_0, F)$, where Q denotes the set of states, $\Sigma_E \subseteq \Sigma$ the set of symbols used in E , Δ the transitions, q_0 the initial state, and F the set of accepting states. The conversion from a regular expression to an NFA can be conducted (for example) using Thompson’s classical algorithm, where we assume that ε -transitions have been (subsequently) removed from M_E . Letting V denote the nodes of G , then the *product graph* $G_E \subseteq (V \times Q) \times (V \times Q)$ of G with respect to E is a directed unlabeled graph defined as follows:

$$G_E = \{((x, q_x), (y, q_y)) \mid \exists p \in \Sigma_E, (x, p, y) \in G \wedge (q_x, p, q_y) \in \Delta\}.$$

The RPQ can then be evaluated by using standard graph search algorithms (e.g., BFS, DFS, etc.) to find paths in the product graph G_E that start from some node $(x, q_0) \in V \times \{q_0\}$ and end in some node $(y, q_f) \in V \times F$ (such that $x = s$ if $s \in \Sigma$, and $y = o$ if $o \in \Sigma$).

3.3 Bit-parallel Glushkov Automata

Consider a regular expression E on alphabet Σ with m occurrences of symbols in Σ . Compared to the classical Thompson’s construction of an NFA from E , Glushkov’s [6, 22] has the disadvantage of generating $\Theta(m^2)$ edges in the worst case, and needing $O(m^2)$ construction time [8]. In exchange, it has various properties that will make it interesting for our purposes:

- (1) The NFA has no ε -transitions.
- (2) The NFA has exactly $m + 1$ states, optimal in the worst case.
- (3) All the transitions arriving at a state have the same label.

These properties imply the following important fact.

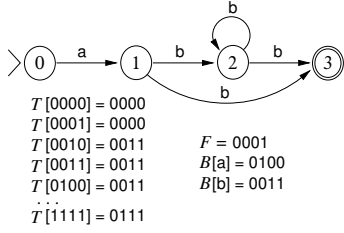


Figure 2: The Gluskov automaton of the regular expression $a/b^*/b$, and its bit-parallel representation below it.

FACT 1. *In a Glushov NFA, the states reached in one step from a set X of states by symbol c are the intersection of those reached from X in one step and those states reached by c from any state.*

Example. The top of Fig. 2 gives the Gluskov automaton for $a/b^*/b$. Take the states $X = \{0, 2\}$. The states $\{2, 3\}$ are reachable from X in one step via b , which is equal to the intersection of the states $\{1, 2, 3\}$ reachable in one step from X via any symbol and the states $\{2, 3\}$ reachable in one step via b from any state. \square

This property enables the *bit-parallel* simulation of the NFA [42]. This simulation represents NFA states as bits in a computer word, so each configuration of active and inactive states (bits set to 1 and 0, respectively), correspond to a state in the DFA according to the classic powerset construction. The simulation operates on all the states in parallel by using the classic arithmetical and logical operations on computer words. Assume for simplicity that the bits of the NFA states fit in a single computer word; we discuss the general case later. Further assume that the alphabet is an integer range $\Sigma = [1.. \sigma]$. The simulation maintains the following variables:

- A computer word D holding $m + 1$ bits tells, at every step, the active NFA states, as discussed. Assume the initial state corresponds to the highest bit.
- A table $B[1.. \sigma]$ of computer words indicates with 1s, at each $B[c]$, the NFA states that are targets of transitions labeled c .
- A table $T[0.. 2^{m+1} - 1]$ stores in $T[X]$, for each possible $(m + 1)$ -bit argument X representing a set of NFA states, the states reachable from states in X in one step, by any symbol.
- A computer word F marks with 1s the final NFA states.

The simulation is then carried out as follows:

- (1) We set $D \leftarrow 2^m$ to activate the initial state.
- (2) If $D \& F \neq 0$, then we have reached a final state and accept the word read (recall that ‘ $\&$ ’ is the bitwise-and).
- (3) If $D = 0$, then we have run out of active states and reject.
- (4) For each input symbol c , we use Fact 1 to update D as follows, such that the new active states are those that are reached from the current ones and also reached by symbol c :

$$D \leftarrow T[D] \& B[c], \quad (1)$$

- (5) Return to point 2.

Example. Fig. 2 shows the Glushkov automaton of $a/b^*/b$ and its bit-parallel representation. Given a string $S = abba$, we initialize $D \leftarrow 1000$ with the initial state 0 activated. We now read $S[1] = a$

and update $D \leftarrow T[1000] \& B[a] = 0100 \& 0100 = 0100$, activating state 1. We read $S[2] = b$ and update $D \leftarrow T[0100] \& B[b] = 0011 \& 0011 = 0011$, indicating that states 2 and 3 are now active. We report here the endpoint of a match since $D \& F = 0011 \& 0001 \neq 0000$. To find other endpoints, we next read $S[3] = b$ and update $D \leftarrow T[0011] \& B[b] = 0011 \& 0011 = 0011$, reporting this position as well. Finally, we read $S[4] = a$ and update $D \leftarrow T[0011] \& B[a] = 0011 \& 0100 = 0000$, so we run out of active states and finish. \square

The space of the simulation is $O(2^m + \sigma)$, instead of the worst-case $O(2^m \sigma)$ of a classical DFA implementation. The tables are built in time $O(2^m)$ by using lazy initialization for B .

A similar simulation can be used to read the text in reverse order [42] by building a table $T'[0.. 2^m - 1]$ where $T'[X]$ marks with 1s the states that can reach some state in X in one step, initializing $D \leftarrow F$ and, for each new symbol c , updating

$$D \leftarrow T'[D \& B[c]], \quad (2)$$

and accepting when $D \& 2^m \neq 0$.

Bit-parallelism uses the RAM model of computation, where all the arithmetical and logical operations over a w -bit word take constant time; it is usual to assume $w = \Theta(\log n)$, where n is the data size. In our case, if $m + 1 > w$, then we need to use $\lceil (m + 1)/w \rceil$ computer words to hold D , F , and every entry of B and T . In this case, all the time and space complexities get multiplied by $O(m/w)$. Furthermore, if we want to avoid the exponential space and time $O(2^m)$, we can split table T vertically into d -bit subtables $T_1, \dots, T_{\lceil (m+1)/d \rceil}$, so that if we partition $X = X_1 \cdots X_{\lceil (m+1)/d \rceil}$, then $T[X] = T_1[X_1] \mid \cdots \mid T_{\lceil (m+1)/d \rceil}[X_{\lceil (m+1)/d \rceil}]$, where ‘ \mid ’ denotes the bitwise-or. This reduces the space to $O((m/d)2^d + \sigma)$ and multiplies the time by $O(m/d)$ instead of $O(m/w)$, for any desired $1 \leq d \leq \min(w, m + 1)$ [42]. We will assume for simplicity that $m = O(w)$ and use $O(2^m)$ space throughout the paper.

3.4 The Ring

The *ring* [4] is a novel representation for a set of triples (s, p, o) , which supports worst-case optimal multijoin queries using the Leapfrog Triejoin algorithm [50]. The ring regards the n triples as a set of n circular strings spo (or pos , or osp) of length 3. It then creates three strings by shifting and sorting the circular strings:

- $L_o[1.. n]$ lists the objects o that (circularly) precede the lexicographically sorted strings spo .
- $L_s[1.. n]$ lists the subjects s that (circularly) precede the lexicographically sorted strings pos .
- $L_p[1.. n]$ lists the predicates p that (circularly) precede the lexicographically sorted strings osp .

The concatenation $L_o \cdot L_s \cdot L_p$ is indeed the Burrows-Wheeler Transform (BWT) [9] of the concatenation of all the triples (with some tweaks, see the original article [4] for details).

With this arrangement, a range in L_o corresponds to a lexicographic interval of triples spo . In particular, a range may represent all the triples with a specific subject s (i.e., strings starting with s), and a smaller range may represent all the triples with subject s and predicate p (i.e., strings starting with sp). A range in L_o can

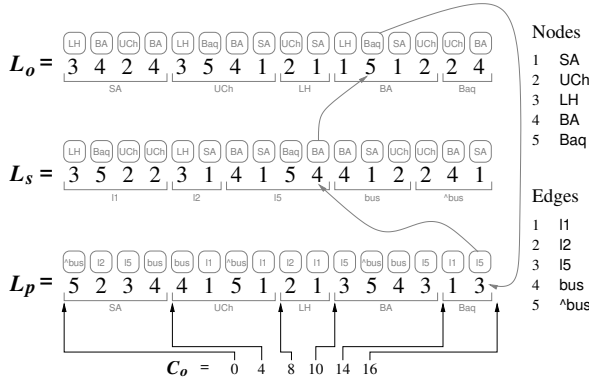


Figure 3: The ring data structure built on the graph of Fig. 1, which we have completed by adding a reverse edge labeled $\hat{\text{bus}}$ for each edge labeled bus (l1, l2 and l5 are bidirectional). We also show how the last triple in L_p is tracked.

also represent a range of subjects $s_b \dots s_e$, and even a subject s followed by a range of predicates $p_s \dots p_e$. Analogously, ranges in L_s correspond to lexicographic intervals of triples pos and ranges in L_p correspond to lexicographic intervals of triples osp . Note that, in the three strings, the range $[1 \dots n]$ represents all the triples and a range of size 1 represents an individual triple.

The ring retrieves triples using so-called *LF-steps*, defined on array L_p (and analogously on L_s and L_o), as follows:

$$\text{LF}_p(i) = C_p[c] + \text{rank}_c(L_p, i), \quad (3)$$

where $c = L_p[i]$, $C_p[c]$ counts the symbols smaller than c in L_p , and $\text{rank}_c(L_p, i)$ counts the number of times c occurs in $L_p[1 \dots i]$. It then holds that the subject of the triple represented at $L_p[i]$ is $L_s[i']$ for $i' = \text{LF}_p(i)$, and the object is $L_o[i'']$ for $i'' = \text{LF}_s(i')$. It further holds that $i = \text{LF}_o(i'')$, where we find the predicate at $L_p[i]$.

Example. Fig. 3 shows the ring for the completion of the graph of Fig. 1, adding reversed edges labeled $\hat{\text{bus}}$. On the right we map the (abbreviated) nodes and edge labels to integers. We write the abbreviated names over the numbers in the sequences L_o , L_s , and L_p for readability. Note that, for example, L_p can be partitioned into the triples osp starting with objects 1 (SA), 2 (UCh), 3 (LH), 4 (BA), and 5 (Baq), which we indicate below the sequence, and whose endpoints are marked in the array C_o , shown on the bottom.

Consider the triple referenced from $L_p[16]$. It refers to the object 5 (Baq) because it belongs to the range $L_p[15 \dots 16] = L_p[C_o[5] + 1 \dots C_o[5 + 1]]$. The value $L_p[16] = 3$ (l5) gives the label of the edge. To find the corresponding subject, we note that this is the fourth 3 (l5) in L_p . Then, if we go to the fourth position in the area of l5 in L_s , $L_s[7 \dots 10]$, which is $L_s[10]$, we learn that the subject is $L_s[10] = 4$ (BA). Indeed, $\text{LF}_p(16) = 10$. Thus, the triple is $\text{BA} \xrightarrow{l5} \text{Baq}$. Further, $L_s[10]$ is the second 4 in L_s , so if we go to the corresponding position $L_o[12]$ (note $\text{LF}_s(10) = 12$) we cyclically find $L_o[12] = 5$ (Baq), the object of the triple. We indeed return to position $L_p[16]$ if we map $L_o[12]$, the second 5 in L_o , to L_p . Again, $\text{LF}_o(12) = 16$. \square

The key to solving multijoins with the ring is the so-called *backward search*, which computes in batch all the LF-steps in a range. Consider a range $L_p[b_o \dots e_o]$ listing, say, all the triples with a specific object o (i.e., all the triples osp for any s and p). The backward search by some specific predicate p gives the range $L_s[b_p \dots e_p]$ corresponding to all the triples with object o and predicate p (i.e., all the triples pos for any s). This is computed with the following formula, which extends the LF-steps (Eq. (3)) to ranges [4, 16]:

$$b_p = C_p[p] + \text{rank}_p(L_p, b_o - 1) + 1, \quad (4)$$

$$e_p = C_p[p] + \text{rank}_p(L_p, e_o). \quad (5)$$

Listing the subjects s in $L_s[b_p \dots e_p]$ then yields all the triples with that specific predicate p and object o , for example.

Example. Continuing our example, let us start from $L_p[11 \dots 14]$, corresponding to object BA. If we apply a backward search step from $b_o = 11$ and $e_o = 14$, on the label 3 (l5) using Eqs. (4) and (5), we obtain $L_s[b_s \dots e_s] = L_s[8 \dots 9] = \langle 1, 5 \rangle$, showing that we arrive at BA by l5 from sources $L_s[8] = 1$ (SA) and $L_s[9] = 5$ (Baq). \square

The ring uses a data structure called a *wavelet tree* [23] to represent each of the sequences L_o , L_s , and L_p , enabling the efficient evaluation of queries like $\text{rank}_p(L_p, i)$.

3.5 Wavelet trees

The wavelet tree represents a string $L[1 \dots n]$ over an alphabet $[1 \dots \sigma]$ as a perfect binary tree with σ leaves, one per symbol, so that the c^{th} left-to-right leaf represents symbol c . Each internal wavelet tree node v that is the ancestor of leaves $c_s \dots c_e$ represents the subsequence $L_{\langle c_s, c_e \rangle}$ of L formed by the symbols in $c_s \dots c_e$. Instead of storing $L_{\langle c_s, c_e \rangle}$, node v stores a bitvector $W_{\langle c_s, c_e \rangle}$, so that $W_{\langle c_s, c_e \rangle}[i] = 0$ iff the leaf representing symbol $S_{\langle c_s, c_e \rangle}[i]$ descends by the left child of v . The leaves are conceptual and not stored. It is not hard to see that all the bitvectors stored at the internal wavelet tree nodes amount to $n \log \sigma$ bits, the same as a plain representation of L (our logarithms default to base 2).

The wavelet tree obtains $L[i]$ in $O(\log \sigma)$ time as follows. Let v be the wavelet tree root, thus it stores bitvector $W = W_{\langle 1, \sigma \rangle}$ where $W[i] = 0$ indicates that $L[i] \in [1 \dots \sigma/2]$; otherwise $L[i] \in [\sigma/2 + 1 \dots \sigma]$ (we assume that σ is a power of 2 for simplicity of presentation). In the first case, $L[i] = L_{\langle 1, \sigma \rangle}[i]$ corresponds to $L_{\langle 1, \sigma/2 \rangle}[i']$, where $i' = \text{rank}_0(W, i)$ and we continue recursively by the left child of v with position i' . In the second case, $L[i]$ corresponds to $L_{\langle \sigma/2+1, \sigma \rangle}[i'']$, where $i'' = \text{rank}_1(W, i)$ and we continue recursively by the right child of v with position i'' .

Operation rank on bitvectors can be done in $O(1)$ time by adding only sublinear space on top of the bitvector [10, 39]. Therefore, in time $O(\log \sigma)$ we arrive at a leaf and determine $L[i]$. The total space of the wavelet tree is $n \log \sigma + o(n \log \sigma) + O(\sigma \log n)$ bits, the latter term for the tree pointers. Note that $O(\sigma \log n)$ also absorbs the space of the arrays C_x used for backward search.

A similar algorithm can be used to compute $\text{rank}_c(L, i)$. We start at the wavelet tree root v and, if c descends by the left child, we recursively go left with $i \leftarrow \text{rank}_0(W, i)$; otherwise we recursively go right with $i \leftarrow \text{rank}_1(W, i)$. When we arrive at the leaf c , the current value of i is the answer. Furthermore, the number of leaf

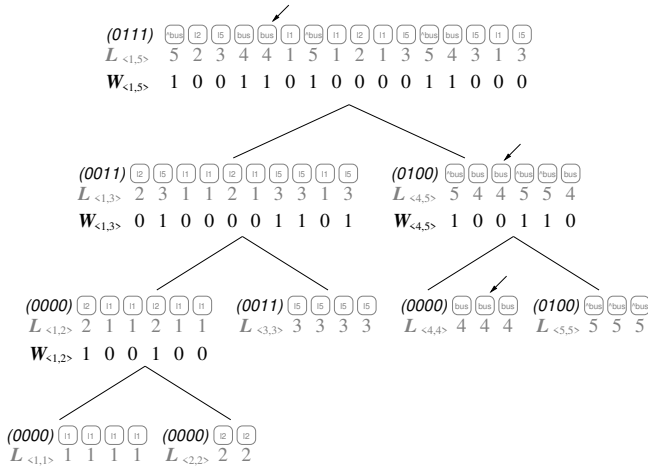


Figure 4: The wavelet tree of the sequence L_p of Fig. 3. The short diagonal arrows track $L[5]$. The slanted bitvectors on the nodes refer to the B entries of the automaton of Fig. 5.

positions to the left of c is precisely $C[c]$, which directly gives the values of the LF and the backward search formulas (Eqs. (3) to (5)).

Example. Fig. 4 shows the wavelet tree of sequence L_p for our running example (ignore the slanted bitvectors for now). To compute $\text{rank}_4(L_p, 5)$, we start at position $i \leftarrow 4$ of the root (the short diagonal arrows track our position along the tree). Since leaf 4 is to the right, we go right and set $i \leftarrow \text{rank}_1(W_{\langle 1,5 \rangle}, 5) = 3$. On the right child of the root, we see that leaf 4 descends to the left, so we go left with $i \leftarrow \text{rank}_0(W_{\langle 4,5 \rangle}, 3) = 2$, arriving at the leaf of 4. Thus $\text{rank}_4(L_p, 5) = i = 2$. The lengths of all the leaves to the left add up to $C_p[4] = 10$, so adding i we obtain position $12 = \text{LF}_p(5)$. \square

Wavelet trees can be used for many other purposes [21, 41]. We will indeed make use of their extended capabilities for our algorithm. A good warmup is the following algorithm to enumerate all distinct symbols in $L[b \dots e]$: We start at the root and descend to the left with the interval $L_{\langle 1, \sigma/2 \rangle}[b' \dots e']$, where $b' = \text{rank}_0(W, b - 1) + 1$ and $e' = \text{rank}_0(W, e)$. We also descend to the right with the interval $L_{\langle \sigma/2+1, \sigma \rangle}[b'' \dots e'']$, where $b'' = \text{rank}_1(W, b - 1) + 1$ and $e'' = \text{rank}_1(W, e)$. We abandon every empty interval and instead report every leaf we arrive at (we later exemplify more complex variants of this algorithm). The total time is then $O(\log \sigma)$ per distinct symbol reported, irrespective of the total number of symbols.

4 OUR APPROACH

We will use part of the ring's structure to navigate backwards all the paths that match a given 2RPQ. More precisely, we use the wavelet trees representing sequences L_p and L_s , as well as all the arrays C_* .

The sets of subjects and objects are equal and correspond to the nodes V in the graph; each node may act as a subject (i.e., edge source) or as an object (i.e., edge target). The set of predicates $P \subseteq \Sigma^{\leftrightarrow}$ corresponds to the edge labels of G^{\leftrightarrow} .

We will first focus on 2RPQs of the form (x, E, o) , where $x \in \Phi$ and $o \in V$. We will build the Glushkov automaton for E and use

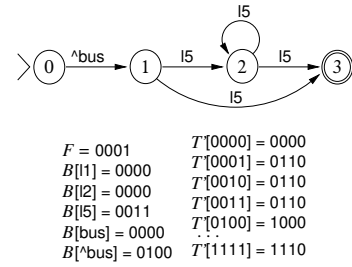


Figure 5: The Glushkov automaton for the regular expression $\hat{\text{bus}}/15^*/15$, its bitvector F and table B , and the transition table T' of its reversed automaton.

it to navigate backwards, from objects towards subjects. Since we use the NFA backwards, we will start from its final states, $D = F$, use the reverse Glushkov simulation of Eq. (2), and report a valid binding $x = s$ at every node $s \in V$ where the initial NFA state is activated. The navigation will start from the range of o in L_p .

This technique also handles 2RPQs of the form (s, E, y) , where $s \in V$ and $y \in \Phi$, by simply reversing E and searching instead for (y, \hat{E}, s) . We will later consider the other kinds of 2RPQs.

We note that since the alphabet of E is P , our vector $B[1 \dots |P|]$ for the bit-parallel NFA simulation is of size $O(|P|)$, but still preprocessing the RPQ takes time $O(2^m)$ with lazy initialization. This adds a working space usage of $O(2^m + |P|)$ on top of the ring.

Example. Assume we are on the metro line 5 (15) at station Baq and want to know what can we reach by following this line and then taking the bus once. The corresponding RPQ is $(\text{Baq}, 15^*/\text{bus}, y)$, and the corresponding reversed regular expression is $\hat{E} = \hat{\text{bus}}/15^*/15$, equivalent to the example $a/b^*/b$ of Fig. 2. We have converted bus to $\hat{\text{bus}}$ to reverse the edge direction (we do not do the same for 15 for simplicity, as all the metro lines bidirectional). Fig. 5 shows the Glushkov automaton for this regular expression; note that $B[\hat{\text{bus}}]$ corresponds to $B[a]$ and $B[15]$ to $B[b]$ in Fig. 2, and that the alphabet of the regular expression is the set of predicates.

To solve the 2RPQ in reverse order, we start from node 5 (Baq) and work backwards. We then start from $L_p[C_o[5] + 1 \dots C_o[6]] = L_p[15 \dots 16]$, and report all the nodes that we can reach in reverse from there that activate the initial state of our automaton, 0. \square

We will virtually traverse the relevant subgraph G'_E of the product graph G_E backwards. To simulate this process, we perform a sequence of (backward) NFA steps, traversing in reverse direction the possible paths ρ that match \hat{E} . The traversal abandons every branch where the NFA runs out of active states. Every time it reaches the initial state we report the current node. Each NFA step starts and ends at a range of L_p corresponding to the current object (initially, o), and is simulated in three parts:

- (1) We find all the predicates labeling edges that lead to the current object. This leads us from the interval in L_p (corresponding to the object) to several intervals in L_s (corresponding to distinct predicates for that object).
- (2) We find the subjects that are sources of edges labeled with each such predicate. This leads us from each interval in L_s

(corresponding to a predicate leading to our object) to several intervals in L_o (corresponding to distinct subjects).

- (3) We regard each of those subjects as an object again, by mapping each resulting range in L_o to the corresponding range in L_p . We only need C_o to do this, not L_o .

After steps 1 and 2, we abandon the branch if the resulting range is empty. After step 2, we perform the NFA transition and abandon the branch if $D = 0$, that is, we run out of active states. We also report the subject if the initial state is active in D .

Note that, in step 1, we are only interested in predicates that lead to some node in G'_E . That is, we want predicates that lead not only to the current object, but also to active NFA states. In step 2, we are only interested in subjects that have not been visited before with the same NFA states, so as to avoid falling into loops of G'_E .

In terms of the product graph, visiting a node s of G with a set D of active NFA states corresponds to traversing *simultaneously* all the nodes of G'_E that combine s with an active state in D . Thus, bit-parallelism enables us to perform significantly less work than classical techniques that visit G'_E node by node. Furthermore, we will combine Fact 1 with the ability of wavelet trees to work on ranges of symbols to carry out steps 1 and 2 in a way that spends time *only on the resulting predicates and subjects*, thereby bounding our time complexity in terms of the subgraph of the size of G'_E , without spending any effort to discard edges that connect G'_E with other nodes of G_E . We now describe each part in detail.

4.1 Part one: Finding predicates from objects

The first part finds the distinct predicates p that lead to (i.e., precede in the osp triples) the current range of objects. We will use the wavelet tree of L_p to discover all the distinct predicates p in $L_p[b_o \dots e_o]$, as described at the end of Section 3.5. From those, however, we are only interested in those predicates p that lead to a currently active NFA state. Those can be efficiently filtered thanks to Fact 1, which lets us confine the influence of p to the table B in the bit-parallel simulation. More precisely, by Eq. (2), we are interested in the predicates p such that $D \& B[p] \neq 0$.

We will enhance the wavelet tree of L_p to efficiently find those predicates. We will have $B[\cdot]$ entries not only for the predicates p , but also for all the other $|P| - 1$ nodes in the wavelet tree of L_p : Let v be a wavelet tree node, then $B[v]$ will be the bitwise-or of the $B[p]$ entries of all the symbols p descending from v .

Example. The $B[\cdot]$ entries for all the nodes of the wavelet tree of L_p are written as slanted bitvectors on the nodes in Fig. 4. Those on the leaves correspond to the entries in Fig. 5, and those on internal nodes to the bitwise-or of their children. \square

This extension is easily built from the $B[p]$ s in $O(m \log |P|)$ time with lazy initialization, by starting with all $B[v] = 0$ and working upwards only from the nonzero entries $B[p]$, doing $B[v] \leftarrow B[v] \mid B[p]$ for every ancestor v of p . The extra space is still $O(|P|)$, and we can conveniently store the entries $B[v]$ in heap order, following the shape of the (perfectly balanced) wavelet tree of L_p .

With this extension of B , we proceed as follows. We start from the root v of the wavelet tree of L_p , with the range $[b \dots e] = [b_o \dots e_o]$ and bitvector D . If $D \& B[v] = 0$, we stop. Otherwise, if v is a leaf

p , then we report the interval $L_s[b \dots e]$. Otherwise, we recursively continue with the left and right children v_l and v_r of v , with the intervals $[b \dots e] = [\text{rank}_0(W, b - 1) + 1 \dots \text{rank}_0(W, e)]$ for v_l and $[b \dots e] = [\text{rank}_1(W, b - 1) + 1 \dots \text{rank}_1(W, e)]$ for v_r .

Example. To start the search from $L_p[14 \dots 15]$ and $D = 0001$, we must first find all distinct values in the range that label transitions leading to an state active in D . We start from the wavelet tree root $v_{\langle 1,5 \rangle}$ of Fig. 4, with the range $L_{\langle 1,5 \rangle}[14 \dots 15]$. We descend to the left child, $v_{\langle 1,3 \rangle}$ since $B[v_{\langle 1,3 \rangle}] \& D = 0011 \& 0001 \neq 0000$ and thus there are relevant transition labels below it. When descending, we map the range to $L_{\langle 1,3 \rangle}[9 \dots 10]$ (because $\text{rank}_0(W_{\langle 1,5 \rangle}, 14 - 1) + 1 = 9$ and $\text{rank}_0(W_{\langle 1,5 \rangle}, 15) = 10$). From $v_{\langle 1,3 \rangle}$, we do not descend to $v_{\langle 1,2 \rangle}$ since $B[v_{\langle 1,2 \rangle}] \& D = 0000 \& 0001 = 0000$ and thus no relevant transition labels descend from it (though there is a 1 in our range $L_{\langle 1,3 \rangle}[9 \dots 10]$ indicating an l1 reaching Baq, it does not lead to active NFA states). Instead, we descend to $v_{\langle 3,3 \rangle}$ because $B[v_{\langle 3,3 \rangle}] \& D = 0011 \& 0001 \neq 0000$. Since it is a leaf, we have found a relevant label (3, i.e., l5) reaching our range (i.e., Baq). Its range is $L_{\langle 3,3 \rangle}[4 \dots 4]$, which added to the number of leaves in l1 and l2 (equivalent to $C_p[3] = 6$) yields the range $L_s[10 \dots 10]$, completing the backward search step for symbol l5 (recall Eqs. (4) and (5)).

On the other hand, we do not descend from $v_{\langle 1,5 \rangle}$ to its right child, $v_{\langle 4,5 \rangle}$, because $B[v_{\langle 4,5 \rangle}] \& D = 0100 \& 0001 = 0000$. Even if we did, we would obtain an empty interval in $L_{\langle 4,5 \rangle}$ because there are no 4s or 5s in $L_{\langle 1,5 \rangle}[15 \dots 16]$. \square

Note that, if $D \& B[v] \neq 0$, then the same holds for at least one of the two children of v . As a consequence, all the wavelet tree nodes we traverse are ancestors of qualifying leaves. Since we spend constant time on each such ancestor, we can bound the total cost of this part by charging $O(\log |P|)$ to each useful predicate p , for which we report the interval $L_s[b_p \dots e_p]$. We do not pay any extra cost on the useless predicates thanks to Fact 1, because we must intersect every $B[p]$ with the same set D of active states.

In terms of the product graph traversal, where we are simultaneously processing all the nodes that combine o with the active states in D ; this technique allows us to obtain all the distinct edges of G'_E that we can traverse from the current nodes of G'_E .

4.2 Part two: Finding subjects from predicates

The second part of the step starts at each of the ranges $L_s[b_p \dots e_p]$ reported by the first part, and traverses the wavelet tree of L_s to find all the distinct subjects s in that range, mapping them to an interval $L_o[b_s \dots e_s]$. By Fact 1, the set of active NFA states will be the same, $D \leftarrow T'[D \& B[p]]$ (Eq. (2)), for all those subjects. If D contains the initial state, we report that subject s starts a path of the 2RPQ (i.e., we report (s, o) as an answer to the query).

Example. In our example, once we obtain the range $L_s[10 \dots 10] = 4$ (BA) from edge label 3 (l5), identifying the edge $\text{BA} \xrightarrow{l5} \text{Baq}$, we update $D \leftarrow T'[D \& B[3]] = T'[0001 \& 0011] = T'[0001] = 0110$, meaning we have activated states 1 and 2 in our NFA (see Fig. 5). This new state D is independent of the subject we arrived at. \square

We need to prevent falling into loops, however: If we arrive at a subject s with a subset of the NFA states we have already visited s

with, we must stop because we are repeating nodes in the product graph. To implement this filter efficiently, we will again exploit Fact 1 and enhance the wavelet tree of L_s .

We will store for each subject s a bitvector $D[s]$ with all the active NFA states we have already reached s with. This adds $O(|V|)$ working space, but can be zeroed in constant time with lazy initialization. Thus, if we arrive at s and $D \mid D[s] = D[s]$, the subject s can be skipped; otherwise we set $D \leftarrow D \& \sim D[s]$ and then $D[s] \leftarrow D \mid D[s]$, where “ \sim ” is the bitwise-not. This leaves in D only the NFA states that are new to s , and also adds to $D[s]$ the new active states we have arrived at s with. We initially mark the states F on the node o where we start the search.

We use the same technique of storing $D[\cdot]$ entries at wavelet tree nodes v of L_s , so as to avoid descending by a branch if all the subjects below it have already been visited with all the active states in D . For this, $D[v]$ must be the intersection of those $D[s]$ cells below v . If $D \mid D[v] = D[v]$, we prune the wavelet tree traversal at node v , otherwise we set $D[v] \leftarrow D \mid D[v]$ and continue by both left and right children. Just as for predicates, there is always a useful descendant leaf s from the nodes v we traverse, and so the total cost is $O(\log |V|)$ per useful subject arrived at.

Not visiting s with a subset of the NFA states of previous visits ensures that we never work more than classical product graph traversals: every time we reprocess a node s of G , we must be including a new NFA state in D (instead, we can be faster because we handle several NFA states together, as explained). Again, we can efficiently filter the subjects with the wavelet tree thanks to Fact 1, because all the subjects s are visited with the same set of states D .

4.3 Part three: Mapping subjects back to objects

In this third part, we report each useful subject s we must consider, with its corresponding state D . In order to proceed with the next step of the simulation, we must map this range of subjects to the same range of nodes seen as objects.

This is easily done with the array C_o , where $C_o[s]$ is the number of symbols smaller than s in L_o . Thus, $L_p[C_o[s] + 1 .. C_o[s + 1]]$ corresponds to the interval of L_p that is aligned to object s .

Then, as explained, we restart part one with each s for which $C_o[s + 1] > C_o[s]$, with state D .

Example. Fig. 6 illustrates the whole process of matching the (2)RPQ $(y, l5^+ / \hat{\text{bus}}, \text{Baq})$, with the NFA of Fig. 5, in the graph of Fig. 1, as represented in Fig. 3. We use a top-down tree to represent the branching of the process, and also show on the top left the states of the product graph G'_E we traverse (backwards). We will use BFS traversal. The top nodes of the tree illustrate what we have already done in previous examples (edge $1 \rightarrow 2$ of G'_E): starting from $L_p[14 .. 15]$ (Baq) and $D = 0001$, we identified the only edge label reaching that node, $l5$, that is relevant in our NFA. Note that the label $l1$ also appears in $L_p[15 .. 16]$ because a transition labeled $l1$ reaches Baq, but $D \& B[l1] = 0000$ because our NFA does not match it; this pruned branch is shown with a dashed arrow leading to an X. We have also seen that the only source of those edges labeled $l5$ is BA, at $L_s[10 .. 10]$, where the NFA is active at states 0110. We do move to BA because $D[\text{BA}] = D[4] = 0000$, so $D = 0110$ contains some unseen NFA states at this node. We then mark $D[4] = 0110$ to indicate that we have already reached BA with those

active NFA states. In part 3 of our process, we find the interval of L_p corresponding to $L_s[10] = 4$ (BA), $L_p[C_o[4] + 1 .. C_o[5]] = L_p[11 .. 14]$, and so complete one step.

Three symbols appear on $L_p[11 .. 14]$ (i.e., three edge labels reach BA), but only $l5$ (left child) and $\hat{\text{bus}}$ (right child) match our NFA. By $l5$ we reach $L_s[8 .. 9]$ using backward search. In this interval we find two sources that, by $l5$, reach BA: SA (left child) and Baq (right child), both with NFA state $D = 0110$ (the same as before). On the other hand, by $\hat{\text{bus}}$, we reach $L_s[16 .. 16]$ using backward search. There we find the only source, SA, that reaches BA, with NFA state $D = 1000$. We process the three sources in BFS order, left to right:

- (1) By $l5$ we reach BA from SA (leftmost tree node in this level). We accept going to SA, as $D[\text{SA}] = D[1] = 0000$ and $D = 0110$ has new states, so we set $D[1] = 0110$. In part 3 we get the interval $L_p[1 .. 4]$ for SA. This is edge $2 \rightarrow 3$ of G'_E .
- (2) By $l5$ we reach BA from Baq (middle tree node in this level). Although we had already seen Baq, it was only with states $D[\text{Baq}] = D[5] = 0001$, so the current state $D = 0110$ has some unvisited NFA states; we set $D[5] = 0111$ and part 3 leads us to $L_p[15 .. 16]$. This is edge $2 \rightarrow 4$ of G'_E .
- (3) By $\hat{\text{bus}}$ we reach BA from SA as well (rightmost tree node in this level). Since $D[\text{SA}] = D[1] = 0110$ and $D = 1000$, we have new states and accept going to SA, setting $D[1] = 1110$. The NFA state is still 1000 (edge $2 \rightarrow 5$ of G'_E), which contains the initial state, so we report SA as a solution to our 2RPQ. We then continue from it, reaching $L_p[1 .. 4]$ using part 3.

Our BFS traversal now branches from each of those three nodes:

- (1) From $L_p[1 .. 4]$ (SA) with $D = 0110$, we find edges labeled $l1$, $l5$, and $\hat{\text{bus}}$ leading to it:
 - (a) Our NFA states are not reachable by $l2$ ($D \& B[l2] = 0000$), so we abandon this branch.
 - (b) By $l5$ we find the source BA, but since $D[\text{BA}] = D[4] = 0110$ and $D = 0110$, we have already visited BA with those active states, so we prune this branch too, avoiding a loop.
 - (c) By $\hat{\text{bus}}$ we reach $L_s[14 .. 14]$ with state $D = 1000$. The only source here is $L_s[14] = 2 = \text{UCh}$. Since $D[\text{UCh}] = D[2] = 0000$, we enter this state and set $D[2] = 1000$ (edge $3 \rightarrow 6$ of G'_E). Furthermore, since D contains the initial state, we report UCh as the second solution to the 2RPQ.
- (2) From $L_p[15 .. 16]$ (Baq) with $D = 0110$, we find edges labeled $l1$ and $l5$ leading to it:
 - (a) Our NFA is not interested in $l1$, so we abandon this branch.
 - (b) By $l5$ we reach BA again, and again we prune the branch to avoid falling into loops, because $D[\text{BA}] = D[4] = 0110$.
- (3) From $L_p[1 .. 4]$ (SA) and $D = 1000$, which we had reported, the NFA has nowhere to go, so we reject all the possible edge labels, $l2$, $l5$, and $\hat{\text{bus}}$. The same happens in the last tree level from $L_p[5 .. 8]$ (UCh) after reporting it, so we finish. \square

4.4 Other kinds of RPQs

The algorithm we have described reports all the subjects (i.e., nodes) $s \in V$ for which there is a path matching E towards some object in the range we started with. If we start with the L_p range for a single object o (i.e., solving (x, E, o) with $x \in \Phi$ and $o \in V$), then the answers to the query are all the pairs (s, o) . We can use this

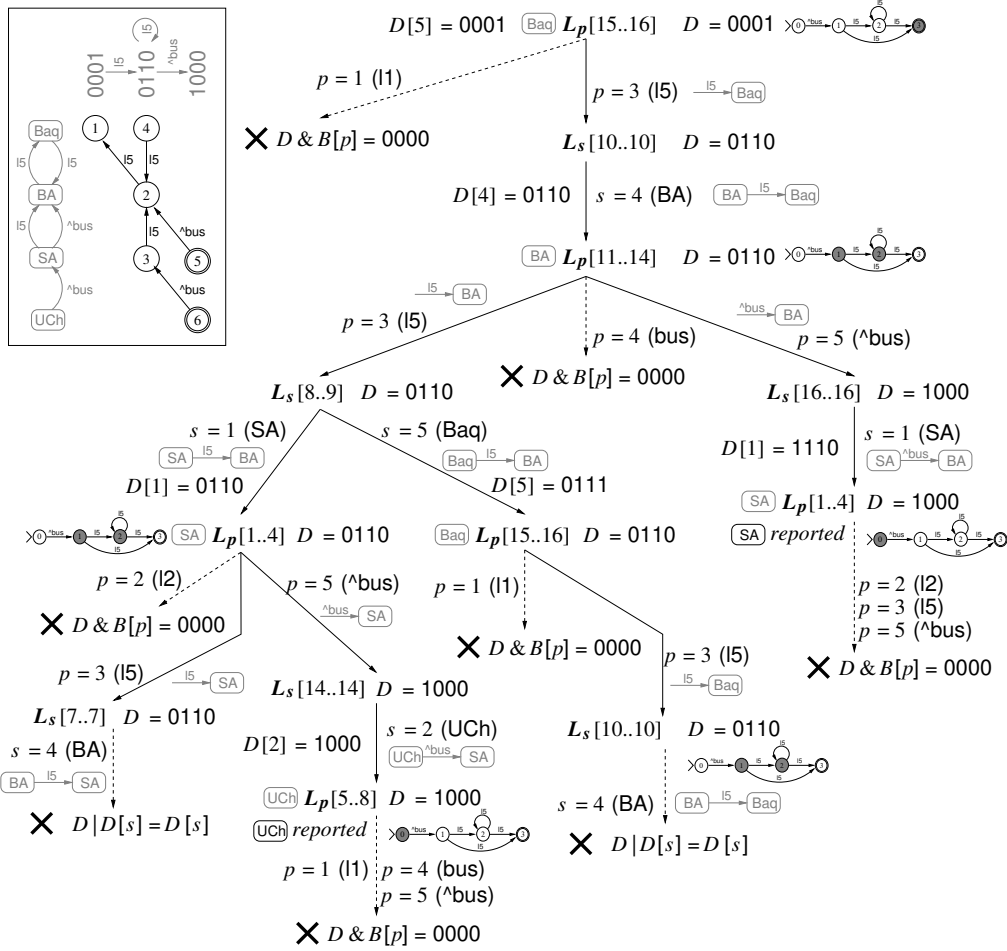


Figure 6: The whole process to match the RPQ of Fig. 5 in our graph of Figs. 1 and 3. On the top left, the visited part of the product graph, showing in the columns the sets D of NFA states we visit (and labeling the arrows for readability).

same algorithm for solving (s, E, y) , where $s \in V$ and $y \in \Phi$, by converting it into (y, \hat{E}, s) (as we did in our running example), so that we find all the objects o reachable from a given subject s .

We can also handle the case where both $s, o \in V$ are fixed, by starting from o and processing \hat{E} , stopping as soon as we reach the state s , or until we run out of active states (or vice versa with E).

The most complex case, (x, E, y) with $x, y \in \Phi$, has variables for both subject and object, where we must find all the pairs (s, o) connected by a path matching E . We could handle this query by launching $|V|$ queries (x, E, o) , one per possible object o , but this would be very inefficient if many objects do not lead to answers (s, o) . Instead, we will use the ability of the BWT and of wavelet trees to work on ranges of symbols, not only on individual ones. Instead of starting with each specific object o , we will start with the full range in L_p . Exactly the same algorithm we have described for queries (x, E, o) , now started with the full range, obtains all the subjects s leading to some object by E . Then, for every subject s we arrived at, we run the RPQ (s, E, y) , and report (s, o) for each object o found in this search. This technique guarantees that we run the queries (s, E, y) only from subjects that will produce some result.

Alternatively, we can first find the objects o that are reachable with E from some subject, and then run only the useful queries (x, E, o) .

The first step of this solution, which starts from the full L_p range, uses the power of the ring to handle a range of nodes simultaneously, effectively traversing in one step a set of nodes of G'_E that relate a number of nodes of G with the same set of NFA states. That is, it provides a second speedup over a classical node-wise traversal of G'_E . The union of the queries (s, E, y) we perform amounts to a second traversal of G'_E .

4.5 Time complexity

The following theorem shows that the cost of our algorithm is essentially bounded by the size of the subgraph G'_E of the product graph G_E induced by the query.

THEOREM 4.1. *Let G be a directed labeled graph over nodes V and an alphabet P of edge labels. Consider an RPQ (x, E, y) where x or y are variables, E has m literals, and the computer word holds $O(m)$ bits. The ring representation of G can return all the matching pairs (s, o) for the RPQ in time $O(2^m + m \log |P| + |G'_E| \log |G|)$, where*

G'_E is the subgraph of the product graph G_E of G and Glushkov's automaton A of E , induced by all the paths ρ from any node (s_μ, i) to any node (o_μ, f) , where μ is an evaluation of (x, E, y) , and i and f are initial and final states of A . The working space of the query is $O(m(2^m + |P| + |V| + \max_\rho))$ bits, where \max_ρ is the length of the longest path ρ . If the computer word holds only $O(m/d)$ bits, the above times are multiplied by d and 2^m becomes $2^{m/d}$.

PROOF. The algorithm virtually visits the nodes of G'_E in reverse order. Let us first consider the query (x, E, o) for $o \in V$. The algorithm starts simultaneously from all the nodes $(o, f) \in G'_E$, for any final NFA state $f \in F$ (let us regard F and D as sets of NFA states). The algorithm preserves the invariant that, if it is at node $v \in V$ with the active NFA states D , then it is the first time it simulates the visit of the node $(v, d) \in G'_E$ for any NFA state $d \in D$. Each transition to new states (v', d') is done in three parts. In the first part, it finds in $O(\log |P|)$ time every distinct label $p \in P$ of edges in G'_E that lead to some state (v, d) for $d \in D$. This cost can be charged to the edges of G'_E that lead to some state (v, d) , because there is at least one edge per resulting label. In the second part, for each label p found, it finds in $O(\log |V|)$ time every distinct node $v' \in V$ such that we reach some current node (v, d) from some unvisited node (v', d') in G'_E via label p (it obtains simultaneously the set D' of all those states d'). We can then charge the cost to the nodes (v', d') of G'_E . The third part takes $O(1)$ time per node arrived at, which becomes the current node in the next iteration.

The total cost is then $O(|G'_E| \log |G|)$ for the traversal. Glushkov's construction takes $O(m^2)$ time to mark all the bits in $B[1..|P|]$ after the constant-time lazy initialization of B . The construction of the bit-parallel tables takes time $O(2^m)$, dominated by table T . Computing the cells B for the internal wavelet tree nodes of L_p adds $O(m \log |P|)$ time, again using lazy initialization, because only $O(m)$ wavelet tree leaves have nonzero cells in B . The lazy initialization of D for the wavelet tree nodes of L_s adds $O(1)$ time.

The working space is $O(m2^m)$ bits for the bit-parallel simulation of the NFA, $O(m(|P| + |V|))$ bits for the tables B/D on the wavelet tree nodes of L_p/L_s , $O(|P| + |V|)$ bits for the compact structures for the lazy initialization of the tables B/D [40, App. C], and $O(m \max_\rho)$ bits for the recursive path traversals carrying the active states D .

If the computer word cannot hold $O(m)$ bits, we split the words into $O(d)$ words of $O(m/d)$ bits each and operate on each word sequentially, thereby multiplying times by $O(d)$.

All the other types of queries (x, E, y) are reduced to the query (x, E, o) we have considered: in case (s, E, y) , where $s \in V$ and $y \in \Phi$, we just reverse the query; in case (x, E, y) where $x, y \in \Phi$, we perform many queries (s, E, y) , which subsume the cost of the initial query that finds the relevant nodes s from any o . Here G'_E is the union of the graphs G'_E for every s . The only case where we may visit more nodes than those in G'_E is the query (s, E, o) with both $s, o \in V$, because we visit nodes that may not lead to s . This is why this case is left out of the theorem. \square

The theorem does not capture the fact that we are able to process several NFA states d simultaneously when traversing the nodes (v, d) of G'_E , thanks to the bit-parallel simulation of the NFA.

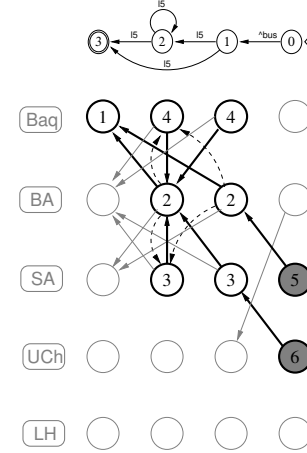


Figure 7: The product graph G_E of the graph of Fig. 1 and the automaton of Fig. 5, highlighting in black the subgraph G'_E that is traversed (backwards) in Fig. 6.

Example. Fig. 7 shows the product graph G_E of our running example, highlighting in bold the nodes and edges of G'_E . The dashed edges also belong to G'_E but we avoid them to prevent loops. The shaded nodes correspond to the reported results. Theorem 4.1 proves that we spend, at worst, logarithmic time per node and edge of G'_E . Comparing the figure with the top-left part of Fig. 6, however, one can see that our simulation processes the nodes of the second and third column of G_E simultaneously (in column 0110 of Fig. 6). We maintained in Fig. 7 the numbering of the nodes of Fig. 6, which helps see the nodes we visit simultaneously. \square

5 IMPLEMENTATION AND EXPERIMENTS

We implemented our scheme in C++11 using the succinct data structures library (SDSL, <https://github.com/simongog/sdsl-lite>). We ran our experiments on an Intel(R) Xeon(R) CPU E5-2630 at 2.30GHz, with 6 cores, 15 MB of cache, and 96 GB of RAM. Our code was compiled using g++ with flags `-std=c++11, -O3, and -msse4.2`.

Benchmark. We test our approach on a real-world benchmark: a Wikidata graph [51] of $n = 958,844,164$ edges and $|V| = 348,945,080$ nodes. This graph has $|S| = 106,736,662$ subjects, $|P| = 5,419$ predicates, and $|O| = 295,611,216$ objects. This dataset occupies 10.7 GB in plain form (i.e., with 32-bit integers for each triple component, or 12 bytes per tuple) and 7.9 GB in packed form (i.e., using $\lceil \log |S| \rceil + \lceil \log |P| \rceil + \lceil \log |O| \rceil$ bits, or 8.625 bytes, per triple).

We compare with the following graph database systems, in terms of the space used for indexing and the time for evaluating RPQs:¹

- Jena:** A reference implementation of the SPARQL standard.
- Virtuoso:** A widely used graph database hosting the public DBpedia endpoint, among others [15].
- Blazegraph:** The graph database system [48] hosting the official Wikidata Query Service [34].

¹While ArangoDB, Neo4j, OrientDB and TigerGraph support various path features – such as bounded traversals, shortest paths, Kleene star, paths with per-edge filters, etc. – to the best of our knowledge they do not support RPQs declaratively.

Table 1: The 20 most popular RPQ patterns in our query log.

1st–7th	#	8th–14th	#	15th–20th	#
v /* c	537	v / v	41	v /? c	22
v * c	433	v * c	36	v + v	17
v + c	109	v v	31	v /+ c	12
c * v	99	v */**/*/* c	28	v v	10
c /* v	95	v ^ v	26	v c	10
v / c	54	v /* v	25	v / ^ v	7
v */* c	44	v * v	25		

Systems are then configured per vendor recommendations, as in previous work [4]. Jena, Virtuoso and Blazegraph all implement RPQs per the semantics of property paths in SPARQL 1.1, whereby fixed-length paths (without * or +) are translated into SPARQL graph patterns without RPQs and evaluated under bag semantics. All systems apply set semantics for arbitrary-length paths, per the SPARQL standard. Jena and Blazegraph implement a navigational BFS-style function called ALP (Arbitrary Length Paths) defined by the SPARQL standard [27], while Virtuoso uses a transitive closure operator implemented over its relational database engine.

In order to test on challenging, real-world RPQs, we extracted all non-trivial RPQs (i.e., not a simple label) from the code-500 (timeout) sections of all seven intervals of the the Wikidata Query Logs [34]. After filtering RPQs mentioning constants not used in the dataset, normalizing variable names, and removing duplicates, this process yielded 1,952 unique queries. All queries are run with a timeout of 60 seconds under set semantics (using DISTINCT in the case of SPARQL) with a limit of 1 million results for comparability (Virtuoso has a hard-coded limit of 2^{20} results). We classify the RPQs of our log into patterns by mapping nodes to constant/variable types and erasing their predicates (keeping only RPQ operators); for example, $(x, p_1/p_2^*, y)$ has the pattern $c /* v, v /* c, \text{ or } v /* v$, depending on whether x and y are constant (c) or variable (v). Table 1 shows the 20 most popular RPQ patterns in our log.

Index construction. We work with a dictionary-encoded version of the graph as described in Section 4, where we complete the graph by adding the reversed edges with inverse labels: If an edge is labeled with predicate p , its reverse edge has predicate $\hat{p} = p + |P|$. This doubles the number of edges and the number of predicates. To construct our index, we build arrays L_s and L_p (and the corresponding C_p and C_o) using a suffix array [4]. We represent L_s and L_p using wavelet matrices [11], a particular implementation of wavelet trees to handle big alphabets efficiently. We use plain bitvectors to implement the wavelet-matrix nodes. Array C_o is represented using a plain bitvector, whereas C_p is represented as a simple array. Our index is constructed in 2.3 hours, using 64.75 GB of RAM.

Implementing queries. We use our generic query algorithm of Section 4, but handle the query patterns $v \hat{v}, v / \hat{v}, v | \hat{v}, v | | \hat{v}$, and v / v more efficiently using just backward search and the extended functionality of wavelet trees: For a variable-to-variable query (x, p, y) (analogously, (x, \hat{p}, y)), we start by extracting all subjects s from $L_s[C_p[p]..C_p[p+1] - 1]$, using the wavelet tree. Then, for each s in that range, we start at range $[C_o[s]..C_o[s] - 1]$ in L_p and carry

Table 2: Index space (in bytes per edge) and some statistics on the query times (in seconds). Row “Timeouts” counts the queries taking over 60 seconds.

	Ring	Jena	Virtuoso	Blazegraph
Space	16.41	95.83	60.07	90.79
Average	3.73	9.93	9.15	6.23
Median	0.15	0.42	0.32	0.15
Timeouts	43	273	154	135
Average c-to-v	0.99	4.99	4.59	4.37
Median c-to-v	0.07	0.22	0.15	0.14
Average v-to-v	18.97	37.46	34.54	16.63
Median v-to-v	8.48	60.00	28.62	0.21

out a backward search step using \hat{p} . This yields the range of L_s containing all values o such that (s, p, o) is a graph edge, so we report (s, o) . Query $(x, p_1|p_2, y)$ (similarly, $(x, p_2|p_3|p_4, y)$) is decomposed into queries (x, p_1, y) and (x, p_2, y) , which are computed as explained before. To detect duplicate pairs (s, o) , we use a hash table (`std::unordered_set` in C++). For query $(x, p_1/p_2, y)$ (similarly, $(x, p_1/\hat{p}_2, y)$) we first find all nodes z that are the target of an edge labeled p_1 , and the origin of an edge labeled p_2 . This is done by intersecting the ranges $L_s[C_p[\hat{p}_1]..C_p[\hat{p}_1 + 1] - 1]$ and $L_s[C_p[p_2]..C_p[p_2 + 1] - 1]$, using the wavelet tree capabilities [21]. Then, for every such z in the intersection, we carry out a backward search for p_1z , to find all nodes s such that (s, p_1, z) is a graph edge. Similarly, we do a backward search for \hat{p}_2z , to find all nodes o such that (z, p_2, o) is a graph edge. Then, for every such s and o we report (s, o) , again avoiding duplicates. Finally, for queries $(x, p_1/(p_2)^*, y)$ we start the search always from p_1 . In general, this filters candidates more efficiently. For all the remaining queries (x, E, y) , we choose to start from the end whose predicate has the smallest cardinality.

We implement array B (used to filter on L_p in Section 4.1) with an array of integers, initially zeroed. We do lazy initialization by setting the values of the different predicates of the query and their wavelet matrix ancestors, and zeroing them again after running the query. Array D , on the other hand, is implemented using the a compact lazy initialization structure [40, App. C], which uses $O(|V|)$ extra bits on top of D . We use 16-bit cells for D , as queries in our log have fewer than 16 predicates (with some few exceptions that use operator $|$, which are handled differently as explained).

Space and query time. Table 2 shows the space usage of the systems we tested, as well as statistics about the whole query process. The ring is the smallest index, using 16.41 bytes per triple. This is about twice the space of the compact representation of the data, consistent with the fact that we duplicate all the edges. Array D , needed at query time, uses 3.09 additional bytes per triple, whereas B uses 9.04×10^{-5} bytes per triple. The total working space usage at query time is 19.50 bytes per triple, 1/3–1/5 of the space used by the other indexes (not considering their extra working space).

Regarding query time, the ring is the fastest on average, being 1.67 times faster than Blazegraph, the next best performer. The ring is also the index with fewest timeouts. On the queries where

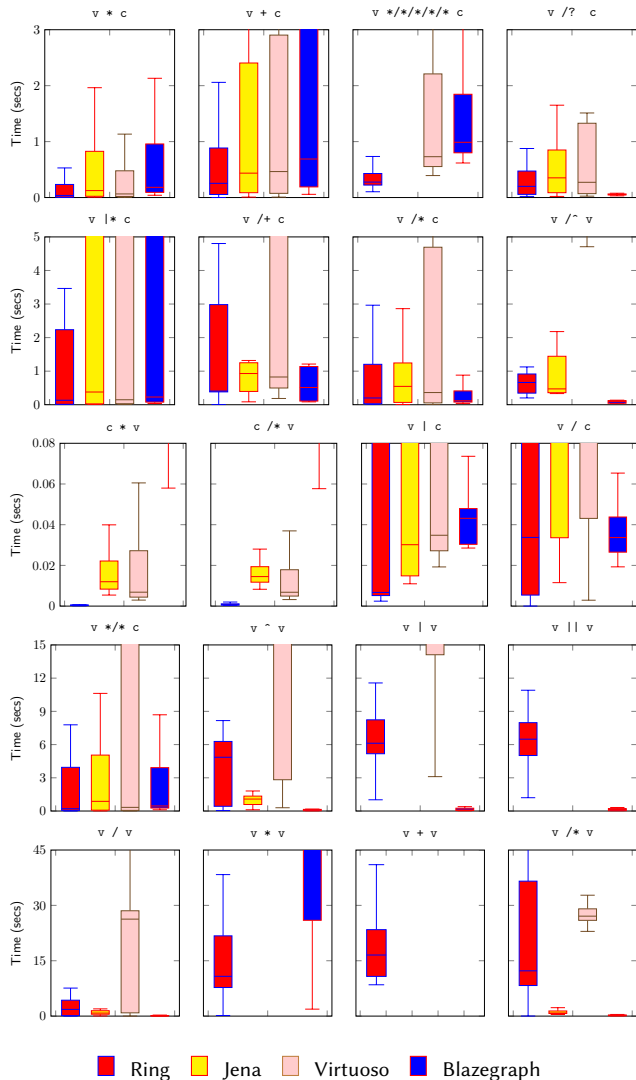


Figure 8: Boxplots for the distribution of query times.

some node is a constant (“c-to-v” in the table, 84.7% of the log), the ring is 4.41 times faster than Blazegraph on average, with only 1 timeout (no system was able to complete that query). The other systems have over 50 timeouts on these queries. For the queries where both nodes are variables (“v-to-v”, 15.3% of the log), the ring is the second best, only 14% slower than Blazegraph on average.

Fig. 8 shows the distribution of query times for the different patterns. Our approach has the best performance in 9 out of 20 patterns, which correspond to 45.39% of the query log. Each of these 9 patterns have at least one * or +. There are only other 3 such patterns, $v/+c$, $v/*c$, and $v/*v$, on which our ring is outperformed by another system. The remaining 8 patterns on which we do not compete are paths of length 1, length 2, and “or” paths. Such paths can be solved as join queries, with more efficient algorithms.

Note that our system works on the integer-encoded triples, whereas others work on the original string values. As shown in

previous work [4], we can encode the strings of this benchmark within just 3 additional bytes per triple and incurring in around 3 extra milliseconds per query, in order to decode the answers.

6 CONCLUSIONS

We have shown how the ring [4], a compact representation of labeled graphs developed to support worst-case optimal graph joins, can be enhanced by combining in a unique way the capabilities of (1) the wavelet trees, to process ranges of graph nodes or labels, and (2) the bit-parallel simulation of Glushkov automata, to handle various NFA states simultaneously, in order to solve regular path queries (RPQs) on the graph. We prove that the cost of the resulting algorithm is proportional to the subgraph of the product graph induced by the query, but our technique is even faster because it is able to process groups of nodes and labels simultaneously. As a result, our index uses 3–5 times less space than the alternatives, while matching or exceeding their performance (on average, our index is the fastest, outperforming the next best by a factor of 1.67).

We have not yet explored strategies for partitioning the NFA at edges with labels that appear infrequently in the graph and then joining the results, as do several techniques described in Section 2. Our techniques do permit running the NFA forwards or backwards from those labels, so this could be explored in future. Furthermore, the wavelet tree offers powerful operations that provide on-the-fly selectivity statistics, which can be used for even more sophisticated query planning. For example, by roughly doubling the space, we can compute in logarithmic time the amount of distinct predicates labeling edges towards a given range of objects, or distinct subjects that are sources of a given range of predicates [20].

Our technique is particularly well-suited to integrate RPQs in SPARQL multijoin queries solved with Leapfrog Triejoin, reusing the same ring data structure [4]. In this case, in addition to the triples of the basic graph patterns, there will be triples of the form (x, E, y) , where E is a regular expression. By treating E as any other relation, the Leapfrog algorithm will choose to first instantiate x (resp., y), and thus will ask for the smallest $x \geq x_0$ (resp., $y \geq y_0$) that has a solution for some y (resp., x). Later, it will instantiate y (resp., x) and will ask for the smallest $y \geq y_0$ (resp., $x \geq x_0$) that has a solution for a concrete value of x (resp., y). The capability of wavelet trees to work on ranges of symbols allows us to find those smallest $x \geq x_0$ or $y \geq y_0$ values efficiently, for example by successive binary partitioning of the range of candidates.

Other requirements are also efficiently met with our data structures. For example, we can easily enforce visiting specific nodes within the regular expression, or that those nodes have specific attribute values, by marking the noncomplying nodes as already visited with the NFA states that enforce those conditions, so they will be avoided in our traversal. The bit-parallel Glushkov simulation also efficiently handles classes of symbols labeling the NFA edges (like $(1|1|2|1|5)$, or negated labels), without building unnecessarily large NFAs; this could be used to support negated property sets defined in SPARQL property paths, or even inference over RDF graphs (e.g., handling virtual disjunctions of inferred properties).

ACKNOWLEDGMENTS

This work was supported by ANID – Millennium Science Initiative Program – Code ICN17_002.

REFERENCES

- [1] Zahid Abul-Basher. 2017. Multiple-Query Optimization of Regular Path Queries. In *International Conference on Data Engineering (ICDE)*. IEEE Computer Society, 1426–1430.
- [2] Renzo Angles, Marcelo Arenas, Pablo Barceló, Peter A. Boncz, George H. L. Fletcher, Claudio Gutiérrez, Tobias Lindaaker, Marcus Paradies, Stefan Plantikow, Juan F. Sequeda, Oskar van Rest, and Hannes Voigt. 2018. G-CORE: A Core for Future Graph Query Languages. In *SIGMOD International Conference on Management of Data*. ACM, 1421–1432. <https://doi.org/10.1145/3183713.3190654>
- [3] Renzo Angles, Marcelo Arenas, Pablo Barceló, Aidan Hogan, Juan L. Reutter, and Domagoj Vrgoc. 2017. Foundations of Modern Query Languages for Graph Databases. *ACM Comput. Surv.* 50, 5 (2017), 68:1–68:40. <https://doi.org/10.1145/3104031>
- [4] Diego Arroyuelo, Aidan Hogan, Gonzalo Navarro, Juan Reutter, Javiel Rojas-Ledesma, and Adrián Soto. 2021. Worst-Case Optimal Graph Joins in Almost No Space. In *ACM International Conference on Management of Data (SIGMOD)*, 102–114.
- [5] Jorge A. Baier, Dietrich Daroch, Juan L. Reutter, and Domagoj Vrgoc. 2017. Evaluating Navigational RDF Queries over the Web. In *ACM Conference on Hypertext and Social Media (HT)*. ACM, 165–174.
- [6] Gerard Berry and Ravi Sethi. 1986. From regular expression to deterministic automata. *Theoretical Computer Science* 48, 1 (1986), 117–126.
- [7] Angela Bonifati, Wim Martens, and Thomas Timm. 2019. Navigating the Maze of Wikidata Query Logs. In *The World Wide Web Conference (WWW)*. ACM, 127–138.
- [8] Anne Brüggemann-Klein. 1993. Regular expressions into finite automata. *Theoretical Computer Science* 120, 2 (1993), 197–213.
- [9] Michael Burrows and David Wheeler. 1994. *A block sorting lossless data compression algorithm*. Technical Report 124. Digital Equipment Corporation.
- [10] David R. Clark. 1996. *Compact PAT Trees*. Ph.D. Dissertation. University of Waterloo, Canada.
- [11] Francisco Claude, Gonzalo Navarro, and Alberto Ordóñez. 2015. The wavelet matrix: An efficient wavelet tree for large alphabets. *Information Systems* 47 (2015), 15–32.
- [12] Dario Colazzo, Vincenzo Mecca, Maurizio Nolé, and Carlo Sartiani. 2018. Path-Graph: querying and exploring big data graphs. In *International Conference on Scientific and Statistical Database Management (SSDBM)*. ACM, 29:1–29:4.
- [13] Isabel F. Cruz, Alberto O. Mendelzon, and Peter T. Wood. 1987. A Graphical Query Language Supporting Recursion. In *SIGMOD International Conference on Management of Data*. ACM Press, 323–330.
- [14] Saumen C. Dey, Victor Cuevas-Vicentín, Sven Köhler, Eric Gribkoff, Michael Wang, and Bertram Ludäscher. 2013. On implementing provenance-aware regular path queries with relational query engines. In *Joint 2013 EDBT/ICDT Conferences*. ACM, 214–223.
- [15] Orri Erling and Ivan Mikhailov. 2009. RDF support in the Virtuoso DBMS. In *Networked Knowledge – Networked Media*. Springer, 7–24.
- [16] Paolo Ferragina and Giovanni Manzini. 2005. Indexing compressed texts. *Journal of the ACM* 52, 4 (2005), 552–581.
- [17] Valeria Fionda, Giuseppe Pirrò, and Mariano P. Consens. 2019. Querying knowledge graphs with extended property paths. *Semantic Web* 10, 6 (2019), 1127–1168.
- [18] George H. L. Fletcher, Jeroen Peters, and Alexandra Poulouvasilis. 2016. Efficient regular path query evaluation using path indexes. In *International Conference on Extending Database Technology (EDBT)*. OpenProceedings.org, 636–639.
- [19] Nadime Francis, Alastair Green, Paolo Guagliardo, Leonid Libkin, Tobias Lindaaker, Victor Marsault, Stefan Plantikow, Mats Rydberg, Petra Selmer, and Andrés Taylor. 2018. Cypher: An Evolving Query Language for Property Graphs. In *SIGMOD International Conference on Management of Data*. ACM, 1433–1445.
- [20] Travis Gagie, Juha Kärkkäinen, Gonzalo Navarro, and Simon J. Puglisi. 2013. Colored range queries and document retrieval. *Theoretical Computer Science* 483 (2013), 36–50.
- [21] Travis Gagie, Gonzalo Navarro, and Simon J. Puglisi. 2012. New Algorithms on Wavelet Trees and Applications to Information Retrieval. *Theoretical Computer Science* 426–427 (2012), 25–41.
- [22] V.-M. Glushkov. 1961. The abstract theory of automata. *Russian Mathematical Surveys* 16 (1961), 1–53.
- [23] Roberto Grossi, Ankur Gupta, and Jeff S. Vitter. 2003. High-order entropy-compressed text indexes. In *Proc. 14th Annual ACM-SIAM Symposium on Discrete Algorithms (SODA)*. 841–850.
- [24] Andrey Gubichev, Srikanta J. Bedathur, and Stephan Seufert. 2013. Sparqling kleene: fast property paths in RDF-3X. In *International Workshop on Graph Data Management Experiences and Systems (GRADES)*. CWI/ACM, 14.
- [25] Andrey Gubichev and Thomas Neumann. 2011. Path Query Processing on Very Large RDF Graphs. In *International Workshop on the Web and Databases (WebDB)*.
- [26] Xintong Guo, Hong Gao, and Zhaonian Zou. 2021. Distributed processing of regular path queries in RDF graphs. *Knowl. Inf. Syst.* 63, 4 (2021), 993–1027.
- [27] Steve Harris, Andy Seaborne, and Eric Prud’hommeaux. 2013. SPARQL 1.1 Query Language. W3C Recommendation. <http://www.w3.org/TR/sparql11-query/>.
- [28] Olaf Hartig and Giuseppe Pirrò. 2017. SPARQL with property paths on the Web. *Semantic Web* 8, 6 (2017), 773–795. <https://doi.org/10.3233/SW-160237>
- [29] Louis Jachiet, Pierre Genevès, Nils Gesbert, and Nabil Layaïda. 2020. On the Optimization of Recursive Relational Queries: Application to Graph Queries. In *SIGMOD International Conference on Management of Data (SIGMOD)*. ACM, 681–697.
- [30] André Koschmieder and Ulf Leser. 2012. Regular Path Queries on Large Graphs. In *International Conference on Scientific and Statistical Database Management (SSDBM) (LNCS)*, Vol. 7338. Springer, 177–194.
- [31] Egor V. Kostylev, Juan L. Reutter, Miguel Romero, and Domagoj Vrgoc. 2015. SPARQL with Property Paths. In *International Semantic Web Conference (ISWC) (LNCS)*, Vol. 9366. Springer, 3–18.
- [32] Jochem Kuijpers, George Fletcher, Tobias Lindaaker, and Nikolay Yakovets. 2021. Path Indexing in the Cypher Query Pipeline. In *International Conference on Extending Database Technology (EDBT)*. OpenProceedings.org, 582–587.
- [33] Baozhu Liu, Xin Wang, Pengkai Liu, Sizhuo Li, and Xiaofei Wang. 2021. PAIRPQ: An Efficient Path Index for Regular Path Queries on Knowledge Graphs. In *International Joint Conference on Web and Big Data (APWeb-WAIM) (LNCS)*, Vol. 12859. Springer, 106–120.
- [34] Stanislav Malyshev, Markus Krötzsch, Larry González, Julius Gonsior, and Adrian Bielefeldt. 2018. Getting the Most Out of Wikidata: Semantic Technology Usage in Wikipedia’s Knowledge Graph. In *International Semantic Web Conference (ISWC)*. 376–394.
- [35] Qaiser Mehmood, Muhammad Saleem, Ratnesh Sahay, Axel-Cyrille Ngonga Ngomo, and Mathieu d’Aquin. 2019. QPPDs: Querying Property Paths Over Distributed RDF Datasets. *IEEE Access* 7 (2019), 101031–101045.
- [36] Alberto O. Mendelzon and Peter T. Wood. 1995. Finding Regular Simple Paths in Graph Databases. *SIAM J. Comput.* 24, 6 (1995), 1235–1258.
- [37] Zhuo Miao, Dan C. Stefanescu, and Alex Thomo. 2007. Grid-Aware Evaluation of Regular Path Queries on Spatial Networks. In *International Conference on Advanced Information Networking and Applications (AINA)*. IEEE Computer Society, 158–165.
- [38] Kento Miura, Toshiyuki Amagasa, and Hiroyuki Kitagawa. 2019. Accelerating Regular Path Queries using FPGA. In *International Workshop on Accelerating Analytics and Data Management Systems Using Modern Processor and Storage Architectures (ADMS@VLDB)*, Rajesh Bordawekar and Tirthankar Lahiri (Eds.). 47–54.
- [39] J. Ian Munro. 1996. Tables. In *Proc. 16th Conference on Foundations of Software Technology and Theoretical Computer Science (FSTTCS)*. 37–42.
- [40] Gonzalo Navarro. 2014. Spaces, Trees and Colors: The Algorithmic Landscape of Document Retrieval on Sequences. *Comput. Surveys* 46, 4 (2014), article 52.
- [41] Gonzalo Navarro. 2014. Wavelet Trees for All. *Journal of Discrete Algorithms* 25 (2014), 2–20.
- [42] Gonzalo Navarro and Mathieu Raffinot. 2005. New Techniques for Regular Expression Searching. *Algorithmica* 41, 2 (2005), 89–116.
- [43] Van-Quyet Nguyen and Kyungbaek Kim. 2017. Efficient Regular Path Query Evaluation by Splitting with Unit-Subquery Cost Matrix. *IEICE Trans. Inf. Syst.* 100-D, 10 (2017), 2648–2652.
- [44] Maurizio Nolé and Carlo Sartiani. 2016. Regular Path Queries on Massive Graphs. In *SIGMOD International Conference on Scientific and Statistical Database Management (SSDBM)*. ACM, 13:1–13:12.
- [45] Anil Pacaci, Angela Bonifati, and M. Tamer Özsu. 2020. Regular Path Query Evaluation on Streaming Graphs. In *SIGMOD International Conference on Management of Data*. ACM, 1415–1430.
- [46] Stephan Seufert, Avishek Anand, Srikanta J. Bedathur, and Gerhard Weikum. 2013. FERRARI: Flexible and efficient reachability range assignment for graph indexing. In *International Conference on Data Engineering (ICDE)*. IEEE Computer Society, 1009–1020.
- [47] Frank Tetzl, Wolfgang Lehner, and Romans Kasperovics. 2020. Efficient Computation of Regular Path Queries. *Datenbank-Spektrum* 20, 3 (2020), 243–259.
- [48] Bryan B. Thompson, Mike Personick, and Martyn Cutcher. 2014. The Big-data@RDF Graph Database. In *Linked Data Management*. Chapman and Hall/CRC, 193–237.
- [49] Oskar van Rest, Sungpack Hong, Jinha Kim, Xuming Meng, and Hassan Chafi. 2016. PGQL: a property graph query language. In *International Workshop on Graph Data Management: Experiences and Systems (GRADES)*. ACM, 7.
- [50] Todd L. Veldhuizen. 2014. Triejoin: A simple, worst-case optimal join algorithm. In *Proc. International Conference on Database Theory (ICDT)*. 96–106.
- [51] Denny Vrandečić and Markus Krötzsch. 2014. Wikidata: A free collaborative knowledgebase. *Communications of the ACM* 57, 10 (2014), 78–85.
- [52] Sarisht Wadhwa, Anagh Prasad, Sayan Ranu, Amitabha Bagchi, and Srikanta Bedathur. 2019. Efficiently Answering Regular Simple Path Queries on Large Labeled Networks. In *SIGMOD International Conference on Management of Data*. ACM, 1463–1480.
- [53] Xin Wang, Guozheng Rao, Longxiang Jiang, Xuedong Lyu, Yajun Yang, and Zhiyong Feng. 2014. TraPath: Fast Regular Path Query Evaluation on Large-Scale RDF Graphs. In *Web-Age Information Management (WAIM) (LNCS)*, Vol. 8485. Springer, 372–383.

- [54] Xin Wang, Junhu Wang, and Xiaowang Zhang. 2016. Efficient Distributed Regular Path Queries on RDF Graphs Using Partial Evaluation. In *International Conference on Information and Knowledge Management (CIKM)*. ACM, 1933–1936.
- [55] Nikolay Yakovets, Parke Godfrey, and Jarek Gryz. 2013. Evaluation of SPARQL Property Paths via Recursive SQL. In *Alberto Mendelzon International Workshop on Foundations of Data Management (AMW) (CEUR Workshop Proceedings)*, Vol. 1087. CEUR-WS.org.
- [56] Nikolay Yakovets, Parke Godfrey, and Jarek Gryz. 2016. Query Planning for Evaluating SPARQL Property Paths. In *SIGMOD International Conference on Management of Data*. ACM, 1875–1889.